Suppression of cavity volume and its oscillation using adaptive geometry

Tezhuan Du *, Yiwei Wang, Chenguang Huang

[1] *Institute of Mechanics, Chinese Academy of Sciences, Beijing, China;*

[2] *University of Chinese Academy of Sciences, China.*

Abstract

Many researchers are interested in cloud cavitation because of its instability which can cause vibration and noise, and even lead to structural damages. In the present work, cavitating flows over a hollow projectile with adaptive shape is simulated to study the effectiveness of re-entrant jet suppression and cloud cavitation control. A fluid-structure coupling model is established to study the performance of adaptive shape on control of cavitation. The proposed model is then applied to simulate cavitating flows over a hollow projectile with the adaptive shape. The adaptive shape is achieved by deformation of an elastic membrane under internal-external pressure difference. The membrane bulges and recovers while cavitation grows and collapses respectively. Conversely, deformation of membrane affects the evolution of cavitation. Different Young modulus is adopted to analysis the interaction between cavitating flow and the elastic membrane. The results show that adaptive shape can reduce the total volume of cavitation and collapse pressure under specific parameters.

Keywords: cavitation suppression, adaptive shape, fluid-structure interaction, collapse pressure

Introduction

Cloud cavitation is the most regular and coherent regime of oscillation of partial cavities. The detachment of bubble cloud will cause significant fluctuation of pressure [1]-[4], and pressure pulse generated by bubble collapse in cloud cavitation is usually considered to be the major cause of structure failure. Many researchers are interested in cloud cavitation because of its instability which can cause vibration and noise, and even lead to structural damages [5]. The instability of a partial cavity is usually considered to be induced by the development of a re-entrant jet [6]. Tanimura [7], Kawanami [8], Pham [9] and Zhang [10] set up barriers in the hydrofoil surface to impede the development of re-entrant jet and control the instability of cavitation.

In the present work, cavitating flows over a hollow projectile with adaptive shape is simulated to study the effectiveness of re-entrant jet suppression and cloud cavitation control.

1. Numerical model

1.1 Problem Description

Simulation of cavitating flow over a cylindrical body with 90° blunt conical head is presented in this study. The cylindrical section of a hollow projectile is covered by an elastic membrane. The boundary conditions are shown in Figure 1.

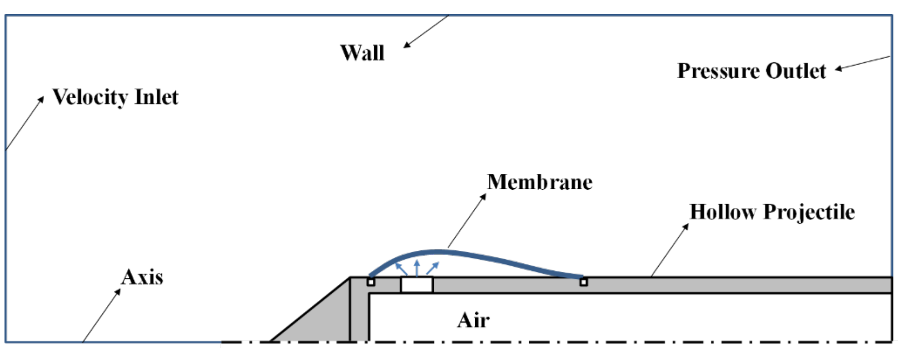

Figure 1: Sketch of the simulation model

*Corresponding Author, Tezhuan Du: dutezhuan@imech.ac.cn

The diameter of the cylinder is D = 37.5 mm, and the thickness of the membrane is h = 0.5 mm. the material of membrane is rubber, density ρ_s = 930 kg/m³, Young's modulus E = 4~16 Mpa. The free-stream velocity is U_∞ = 18 m/s and the ambient pressure is 101325pa. Physical properties of liquid, vapor and air are listed as follows:

Table 1. Physical properties of working fluids

Phase	Density (kg/m^3)	Viscosity (kg/m-s)
liquid	998.2	1.00×10^{-3}
vapor	0.5542	1.34×10^{-5}
air	ideal gas	1.79×10^{-5}

The saturation pressure of water is set as 2367pa. The corresponding cavitation number and Reynolds number are Σ = 0.611 and Re = 6.75×10^5, respectively.

The 2-D axisymmetric model is utilized in the simulation. The coupling model consists of a fluid solver, a structure solver and a data interface.

1.2 Flow Model

The flow field is divided by the membrane into two regions. The outer flow is cavitating flow, and the inner flow is expansion and contraction of gas. The approach for cavitating flows consists of unsteady Reynolds Averaged Navier-Stokes equations of mixture phase, continuity equation of vapor phase and "full cavitation model" developed by Singhal et al [11].

$$\frac{\partial \rho_m}{\partial t} + \nabla \bullet (\rho_m \vec{u}_m) = 0 \tag{1}$$

$$\frac{\partial}{\partial t}(\rho_m \vec{u}_m) + \nabla \bullet (\rho_m \vec{u}_m \vec{u}_m) = -\nabla p + \nabla \bullet [\mu_m (\nabla \vec{u}_m + \nabla \vec{u}_m^T)] + \nabla \bullet (-\rho_m \overline{\vec{u}'_m \vec{u}'_m}) \tag{2}$$

where $\mu_m = \alpha_v \mu_v + \alpha_g \mu_g + (1 - \alpha_v - \alpha_g)\mu_l$ is the equivalent viscosity of the mixture phase. In the present work, the Modified RNG $k-\varepsilon$ model [12] is used to simulate the turbulent effect on cavitation. The

For inner flow, based on quasi-static hypothesis, the pressure is assumed uniform inside projectile, which is given by:

$$p_{in} = \frac{p_0 V_0}{(V_0 + dV)} \tag{3}$$

where p_0 is initial pressure inside, V_0 is initial volume of air inside, dV is volume difference.

1.3 Structural Model

2D axisymmetric is utilized in the present work, the mode shapes and modal frequencies are given by:

$$\phi_j = \sqrt{\frac{2}{\rho A L}} \sin \frac{j\pi x}{L} \tag{4}$$

$$\omega_j = \frac{j\pi}{L}\sqrt{\frac{E}{\rho}} \tag{5}$$

where ϕ_j is the jth natural vibration mode, x is axial coordinate, ρ is the density of membrane, E is Young's modulus, A is the cross-sectional area of the membrane, and L is the length of the membrane. The circumferential constraint can be equivalent to the modified elastic modulus.

The radial displacement of the membrane is calculated using modal superposition method.

$$u_n(x) = \sum q_{j,n} \phi_j \tag{6}$$

where $q_{j,n}$ is the corresponding modal displacement at the nth time step.

Owing to the existence of the wall of the projectile, radial displacement of the membrane is subject to the following constraint condition:

$$u_n(x) \geq 0 \tag{7}$$

In the present work, only the first three orders of vibration mode are considered. The Runge-Kutta method is adopted to solve equation (6) in time domain [13].

1.4 Coupling method

Loose coupling approach is employed in this paper. The flow field and solid field are simulated respectively. The interaction between these two fields is achieved by exchanging the data through the fluid-solid interface at every time step. The data exchange through the interface includes the following two parts:

(1). Mapping the hydro force onto the solid mesh from the fluid mesh.

(2). Mapping the displacement of solid onto fluid mesh from the solid mesh.

In the present work, FLUENT was used to simulate the cavitating flow and SIMPLE algorithm was adopted to solved the velocity-pressure coupled system. The structure solver and coupling interface were programmed and linked to FLUENT as user-defined functions (UDFs). Memory swapping was implemented for data exchange which could enhance the simulation efficiency. The block diagram of fluid-structure coupling method is shown in Figure 2.

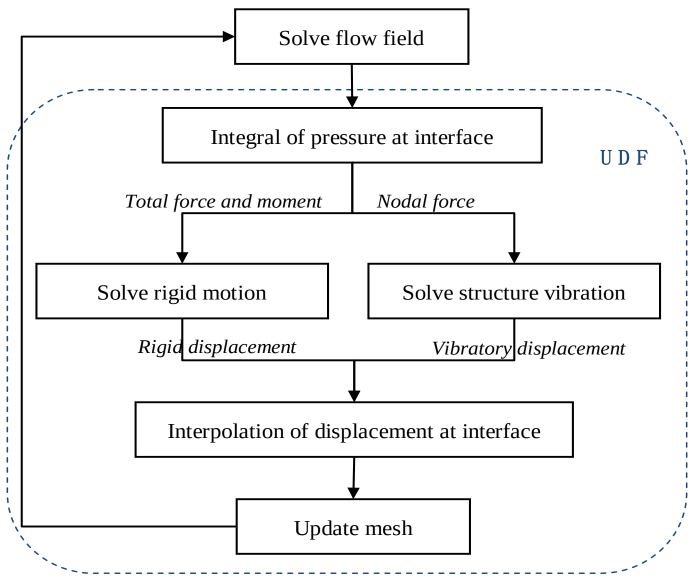

Figure 2: Block diagram of fluid-structure coupling method

2. Results

2.1 Influences of shape deformation on cavitation

Owing to the internal-external pressure difference, the membrane bulges, and recovers while cavitation grows and collapses respectively. Conversely, deformation of membrane affects the evolution of cavitation. Different Young modulus is adopted to analyze the interaction between cavitating flow and the elastic membrane. Figure 3 illustrates that the q_1 is an order of magnitude larger than q_2 and q_3, which indicates that the first order mode shape plays a primary role in deformation.

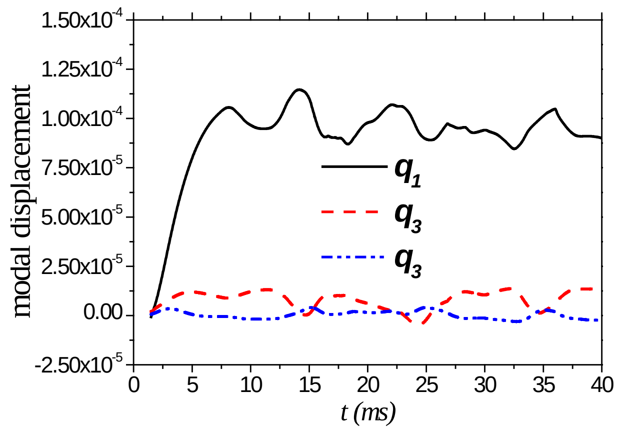

Figure 3: Modal displacement with E = 10 Mpa

In this paper, the total volume of cavitation is chosen to indicate the effect of cavitation suppression. Non-dimensional volume and non-dimensional time are defined as $V' = \frac{V_{total}}{\frac{1}{4}\pi D^3}$ and $t' = \frac{tU_\infty}{D}$ respectively.

The results show that adaptive shape can reduce the total volume of cavitation and collapse pressure under specific parameters. The vibration amplitude of membrane increase with the decreases of Young's modulus. However, the outlines of cavitation area (Figure 4 dash curve) almost the same. It indicates that the total volume of cavitation decrease with the decreases of Young's modulus (Figure 5). While the deformation of membrane exceeds the outline of cavitation area (E = 4 Mpa), newly attached cavitation will appear behind the hump (Figure 6). In this case, the total volume of cavitation will increase.

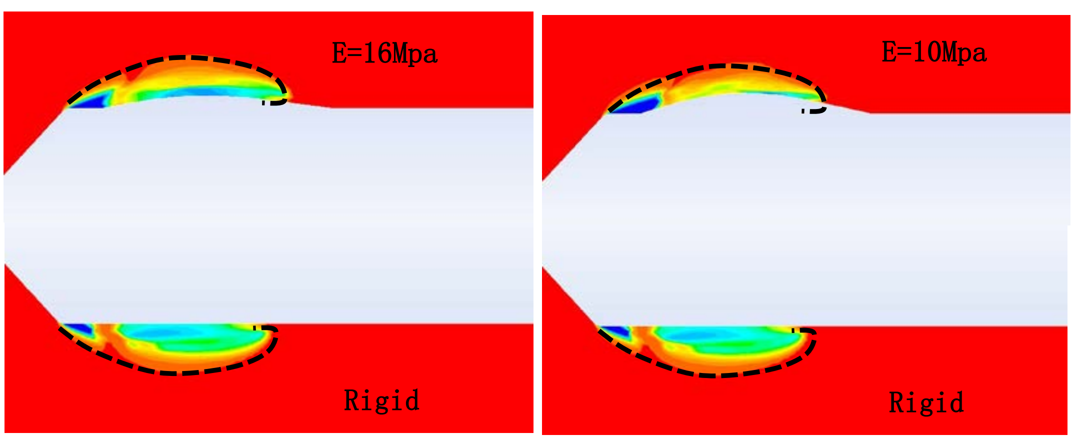

Figure 4: Cavitation outlines with different Young’s modulus.

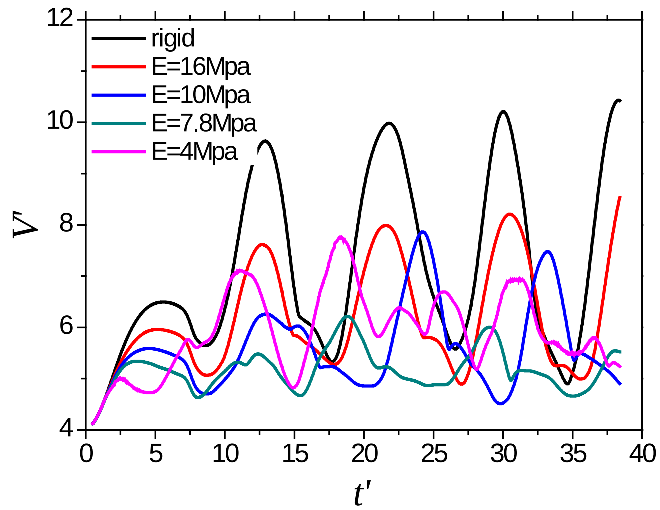

Figure 5: Comparisons of cavitation volume with different Young's modulus.

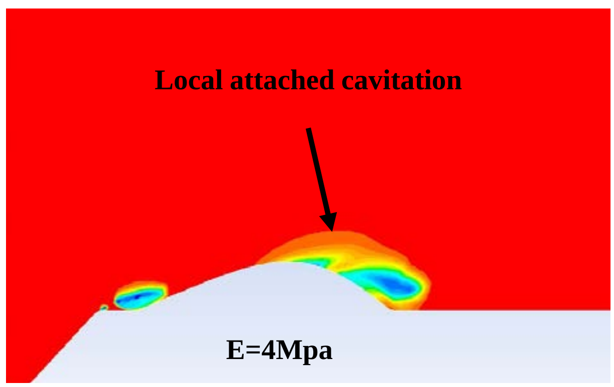

Figure 6: Growth of local attached cavitation (E = 4 Mpa).

2.2 Influence of deformation on pressure

There are two mechanisms for generating pressure pulses: the re-entrant jet meets the main flow at the shoulder of the projectile and the collapse of the detached cavity. Figure 7 shows that deformation of the membrane can significantly reduce the max pressure $p' = \dfrac{p_{\max}}{\frac{1}{2}\rho_L U_\infty^2}$ in the flow field on certain conditions (E = 7.8 Mpa and E = 10 Mpa), especially the pressure pulse generated by re-entrant. It's because the re-entrant jet is restrained by the deformation of the membrane. Meanwhile, the volume of the detached cavity is reduced which may lead to lower collapse pressure.

However, more pressure peaks are generated due to the appearance of locally attached cavitation while E = 4 Mpa.

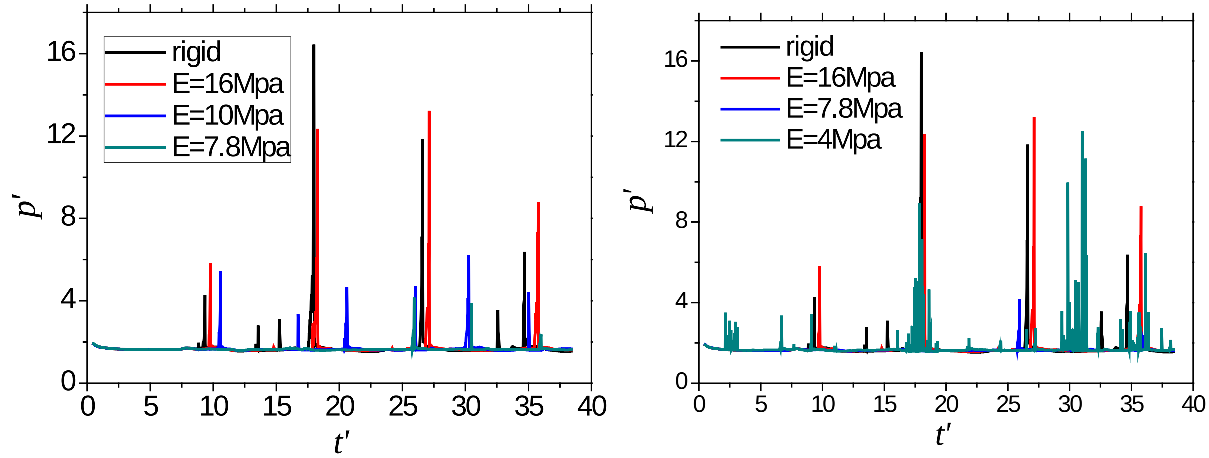

(a) (b)

Figure 7: Comparisons of max pressure with different Young's modulus.

3. Conclusion

In the present work, a fluid-structure coupling model is established to study the performance of adaptive shape on control of cavitation. Different Young modulus is adopted to analyze the interaction between cavitating flow and the elastic membrane. The simulation results show that:

1. The membrane bulges and recovers while cavitation grows and collapses respectively under internal-external pressure difference.

2. The total volume of cavitation decrease with the decreases of Young's modulus. However, while the deformation of membrane exceeds the outline of cavitation area (E = 4 Mpa), the total volume of cavitation will increase due to the appearance of locally attached cavitation.

3. The deformation of the membrane can restrain the development of re-entrant and reduce the volume of the detached cavity, and hence significantly reduce the max pressure in the flow field on certain conditions (E = 7.8 Mpa and E = 10 Mpa).

Acknowledgements: The authors acknowledge the financial support from the National Natural Science Foundation of China (11402276)

References

[1] Arndt R E A, Balas G J, Wosnik M (2005), *Control of Cavitating Flows: A Perspective*, Jsme International Journal, 48(2):334-341.

[2] Huang B, Ducoin A, Yin L Y (2013), *Physical and numerical investigation of cavitating flows around a pitching hydrofoil*, Physics of Fluids, 25(10):213-52.

[3] Ji B, Luo X, Peng X, Wu Y, Xu H (2012), *Numerical analysis of cavitation evolution and excited pressure fluctuation around a propeller in non-uniform wake*, International Journal of Multiphase Flow, 43(43):13-21.

[4] Yu C, Wang Y, Huang C, Wu X and Du T (2017), *Large eddy simulation of unsteady cavitating flow around a highly skewed propeller in non-uniform wake*, Journal of Fluids Engineering, 139: 041302.

[5] Yamamoto K (1991), *Instability in a cavitating centrifugal pump*. JSME Int. J. Ser. II, 34:9~17.

[6] Callenaere M, Franc J P, Michel J M and Riondet M (2001), *The cavitation instability induced by the development of a re-entrant jet*, Journal of Fluid Mechanics, 444(444):223-256.

[7] Tanimura M, Kato H (1995), Maeda M et al, *Mechanism of cloud cavitation and its control*, International Journal of JSME(B), 178:41~50.

[8] Kawanami Y, Kato H, Yamaguchi H, Tanimura M, Tagaya Y (1997), *Mechanism and control of cloud cavitation*, Journal of Fluid Engineering, 119(4) :788–794.

[9] Pham T M, Larrarte F, Fruman D H (1999), *Investigation of unsteady sheet cavitation and cloud cavitation mechanisms*, Journal of Fluid Engineering, 121(2):289~296.

[10] Zhao W G, Zhang L X, Shao X M, Deng J (2010), *Numerical study on the control mechanism of cloud cavitation by obstacles*, Proceedings of the 9th International Conference on Hydrodynamics.

[11] Singhal A K, Athavale M M, Li H, Jiang Y (2002), *Mathematical Basis and Validation of the Full Cavitation Model*, Journal of Fluids Engineering, 124(3): 617-624.

[12] Stutz B, Reboud J L (1997) , *Two-phase flow structure of sheet cavitation*, Physics of Fluids, 9(12):3678-3686

[13] Ascher U M, Ruuth S J, Spiteri R J (1997), *Implicit-explicit Runge-Kutta methods for time-dependent partial differential equations*, Elsevier Science Publishers B. V.